SUPPLEMENTAL INFORMATION

Translation initiation factor 3 regulates switching between different modes of ribosomal subunit joining

Daniel D. MacDougall and Ruben L. Gonzalez, Jr.

Columbia University, Department of Chemistry, 3000 Broadway, New York, NY, 10027, USA

Correspondence to Ruben L. Gonzalez Jr: *Columbia University, Department of Chemistry, 3000 Broadway, Havemeyer Hall - MC 3126, New York, NY 10027, USA; Tel.: (212) 854-1096; Fax: (212) 932-1289; Email: rlg2118@columbia.edu*

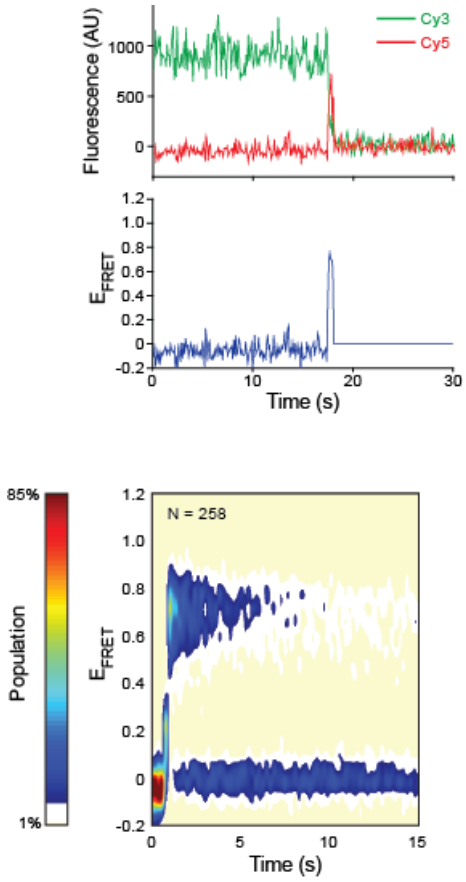

Figure S1: Subunit joining to 30S IC_{+IF3} at higher ionic strength. The majority of smFRET experiments reported in this work were performed in a previously reported variant of Tris-polymix buffer[1]. When experiments were performed in Tris-polymix buffer with higher ionic strength (50 mM Tris-OAc, $pH_{25°C}$ = 7.5, 100 mM KCl, 5 mM NH_4OAc, 0.5 mM $Ca(OAc)_2$, 0.1 mM EDTA, 1% β-D-glucose, 5 mM putrescine dihydrochloride, 1 mM spermidine free-base, 6 mM β-mercaptoethanol, and 15 mM $Mg(OAc)_2$), subunit joining events were followed by rapid loss of the fluorescence signal in a large fraction of the E_{FRET} versus time trajectories. This signal loss was attributed to dissociation of (Cy3)IF2-GDP from the 70S IC. Top Row: Sample Cy3 and Cy5 fluorescence intensity versus time trajectory and the corresponding E_{FRET} versus time trajectory for stopped-flow delivery of (Cy5)50S subunits to (Cy3)30S IC_{+IF3} in higher ionic strength Tris-polymix buffer. (Cy3)30S IC_{+IF3}s for these experiments were assembled on an *in vitro* transcribed mRNA (5'-GG**CAACCUAAAACUUACACA**AAUUAAA<u>AAGGA</u>*AAUAGAC***<u>AUG</u>**UUCAAAGUCGAAAAAUCUACUGCUG-3', where the region complementary to the 3'-biotinylated DNA is bold, the Shine-Dalgarno sequence is underlined, the spacer region is in italics, and the start codon is bold and underlined) hybridized to a complementary 3'-biotinylated-DNA (5'-TGTGTAAGTTTTAGGTTGATTTG-Biotin-3');. Following surface immobilization of (Cy3)30S IC_{+IF3}s in the presence of IF1 (0.9 μM), IF3 (0.9 μM), and GTP (1 mM), imaging buffer containing (Cy5)50S subunits (20 nM), IF1 (0.9 μM), and GTP (1 mM) was stopped-flow delivered into the flowcell. Bottom row: Post-synchronized time evolution of

population FRET histogram, generated by synchronizing individual smFRET versus time trajectories to the first subunit joining event and subsequently superimposing the synchronized trajectories. The number of trajectories used to generate the histogram is indicated by “N”. Contours are plotted from tan (lowest population, ≤1% of counts in the most populated bin) to red (highest population, ≥85% of counts in the most populated bin).

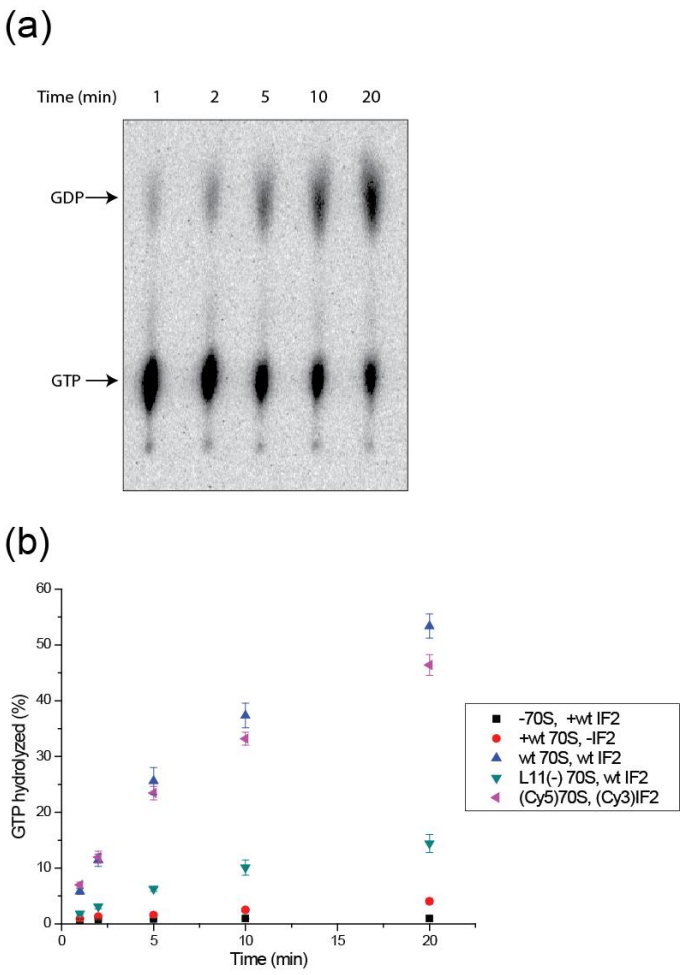

Figure S2: GTP hydrolysis assay. Reactions were performed by mixing 30S and 50S subunits (0.4 μM each, when included), IF2 (0.8 μM, when included), and a mixture of 25 μM GTP-0.25 nM [α-^{32}P]GTP in Tris-polymix buffer (10 mM Tris-OAc, $pH_{25°C}$ = 7.5, 20 mM KCl, 1 mM NH_4OAc, 0.1 mM $Ca(OAc)_2$, 0.1 mM EDTA, 5 mM putrescine-HCl, 1 mM spermidine free-base, 1% β-D-glucose, 15 mM $Mg(OAc)_2$, and 6 mM β-mercaptoethanol). Reactions were incubated at room temperature and quenched with EDTA at the indicated time points. Hydrolyzed [α-^{32}P]GDP was subsequently separated from [α-^{32}P]GTP by thin layer chromatography (TLC) and the percent GTP hydrolyzed was quantified by phosphorimaging as previously described[2]. See Materials and Methods for further details. **(a)** Sample TLC image showing conversion of [α-^{32}P]GTP to [α-^{32}P]GDP. **(b)** Time course of reaction with different combinations of IF2 and ribosomes. wt 70S: 30S and 50S subunits from the wild-type strain NVD001[3,4]; wt IF2: recombinant γ-isoform of *E. coli* IF2; L11(-) 70S: 30S and 50S subunits from the L11-deletion strain NVD005[3,4]; (Cy5)70S: 30S subunits from NVD005 and 50S subunits from NVD005 reconstituted with (Cy5)L11; (Cy3)IF2: Cy3-labeled IF2(S672C). The approximately four-fold reduction in multiple-turnover GTP hydrolysis observed in the absence of L11 is consistent with previous reports[5]. Error bars represent standard deviations from three independent measurements.

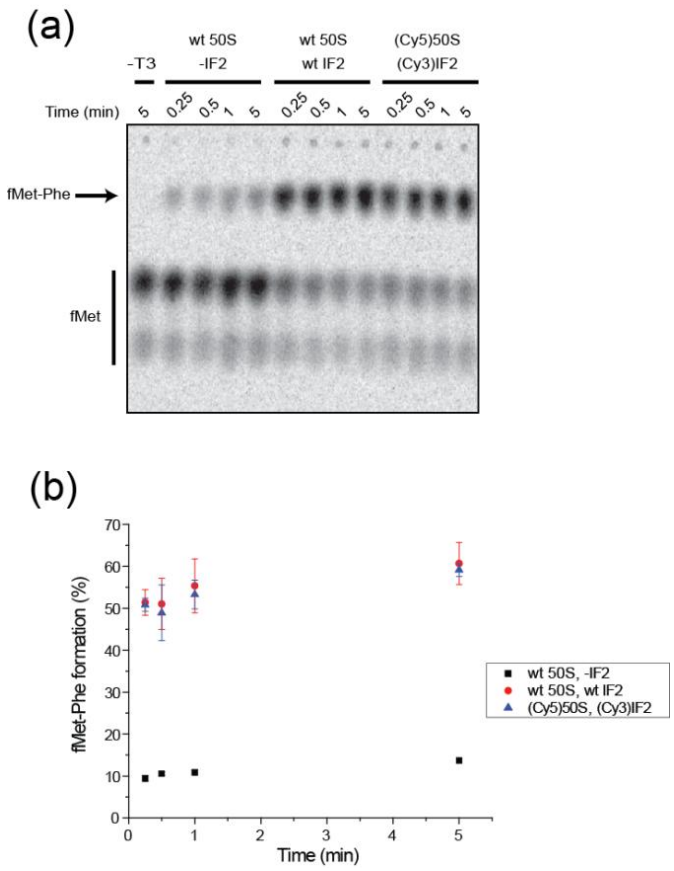

Figure S3: Initiation dipeptide formation assay. Pre-formed 30S ICs were first prepared containing IF1, IF2 (when included), GTP , non-biotin mRNA , 30S subunits , and [^{35}S]fMet-tRNA^{fMet} in Tris-polymix buffer (10 mM Tris-OAc, $pH_{25°C}$ = 7.5, 20 mM KCl, 1 mM NH_4OAc, 0.1 mM $Ca(OAc)_2$, 0.1 mM EDTA, 5 mM putrescine-HCl, 1 mM spermidine free-base, 1% β-D-glucose, 15 mM $Mg(OAc)_2$, and 6 mM β-mercaptoethanol). Next, two mixtures were prepared in the same Tris-polymix buffer, one containing the pre-formed 30S ICs and the other containing 50S subunits and pre-formed EF-Tu(GTP)Phe-tRNA^{Phe} ternary complex (TC). These mixtures were incubated separately for 5 min at room temperature and then combined to start the reaction. The final reaction volume was 10 μL and contained final concentrations of 150 nM 30S ICs, 225 nM 50S subunits, and 600 nM T3 (when included). Reactions were incubated at room temperature and quenched with 1M KOH at the indicated time points, and [^{35}S]fMet-Phe dipeptide product was separated from unreacted [^{35}S]fMet using electrophoretic thin layer chromatography (eTLC)[6]. Unreacted [^{35}S]fMet migrates as two spots corresponding to oxidized and reduced forms of the amino acid. In this assay, formation of [^{35}S]fMet-Phe dipeptide requires subunit joining, binding of TC to the resulting 70S IC, accommodation of Phe-tRNA^{Phe} into the ribosomal aminoacyl-tRNA binding (A) site, and peptide bond formation. See Materials and Methods for further details. **(a)** Sample eTLC image. wt 50S: 50S subunits from strain NVD001; (Cy5)50S: 50S subunits from strain NVD005 reconstituted with (Cy5)L11; wt IF2: recombinant γ-isoform of *E. coli* IF2; (Cy3)IF2: Cy3-labeled IF2(S672C). For each

experiment, 30S subunits used to prepare 30S ICs and 50S subunits were from the same strain. All experiments contained 30S ICs, 50S subunits, and T3 unless otherwise indicated. **(b)** Quantification of time courses. Error bars represent the standard deviation from three independent measurements.

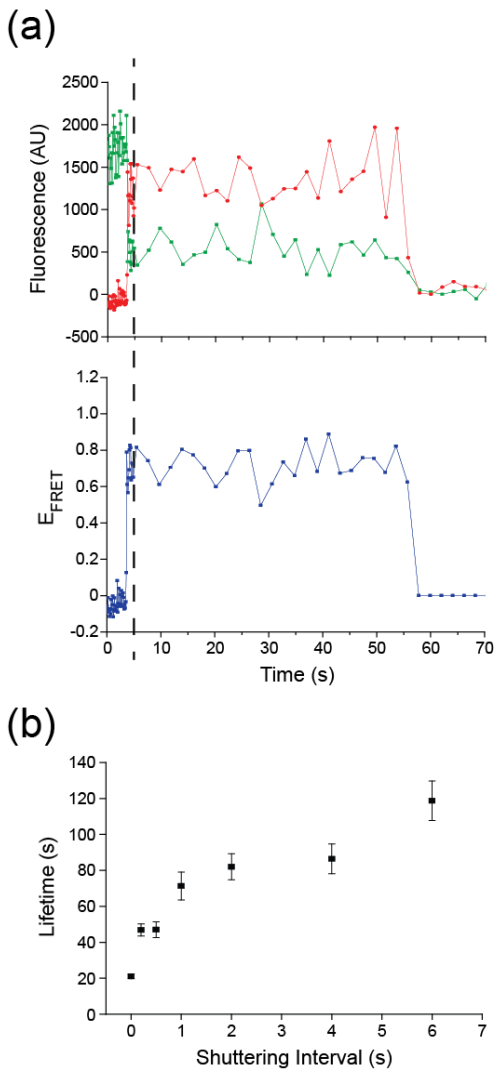

Figure S4: Measurement of the lifetime of the aggregate non-zero FRET state for subunit joining to 30S IC$_{-IF3}$ using shuttering. Upon delivery of (Cy5)50S subunits to surface-immobilized (Cy3)30S IC$_{-IF3}$s, the first five seconds of data were recorded continuously at a frame rate of 10 s^{-1}. At the five-second mark (indicated by the vertical dashed line) the excitation laser light was shuttered and 100 ms frames were collected at regular intervals. **(a)** Sample Cy3 and Cy5 fluorescence intensity versus time trajectory and the corresponding E_{FRET} versus time trajectory collected using a shuttering interval of 2 s. **(b)** Plot of the lifetime of the aggregate non-zero FRET state subsequent to subunit joining versus shuttering interval. Lifetimes were obtained by constructing survival probability plots from dwell times in the aggregate non-zero FRET state from hundreds of single molecules and fitting with a single-exponential decay. Error bars represent the mean and standard deviation obtained from bootstrapping analysis.

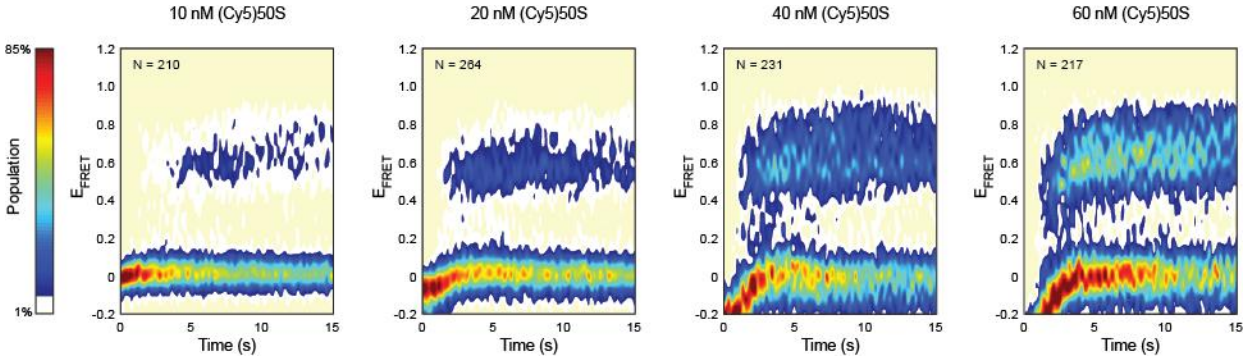

Figure S5: Subunit joining to 30S IC_{+IF3} at different 50S subunit concentrations. Time evolution of population FRET histograms for delivery of 10, 20, 40, or 60 nM (Cy5)50S subunits to surface-tethered (Cy3)30S IC_{+IF3}. The imaging buffer delivered into the flowcell additionally contained IF1 (0.9 μM) and GTP (1 mM), but did not contain IF3. Time evolution of population FRET histograms were constructed by superimposing hundreds of individual E_{FRET} versus time trajectories. The number of trajectories used to generate the histograms is indicated by "N". Contours are plotted from tan (lowest population, ≤1% of counts in the most populated bin) to red (highest population, ≥85% of counts in the most populated bin) according to the color bar on the left.

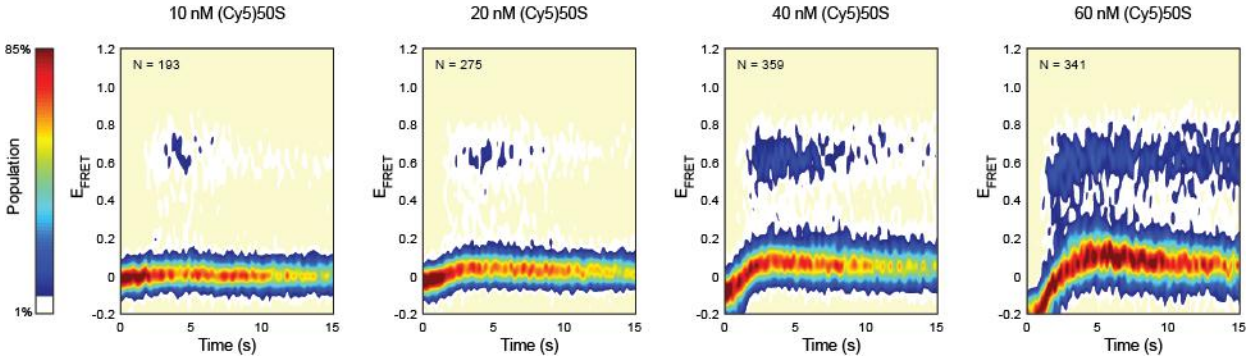

Figure S6: Subunit joining to 30S IC_{+IF3} with free IF3 in the imaging buffer and at different 50S subunit concentrations. Time evolution of population FRET histograms for delivery of 10, 20, 40, or 60 nM (Cy5)50S subunits to surface-immobilized (Cy3)30S IC_{+IF3}. The imaging buffer delivered into the flowcell contained IF1 (0.9 μM), IF3 (0.9 μM), and GTP (1 mM). Data are plotted as in Supplemental Figure 5.

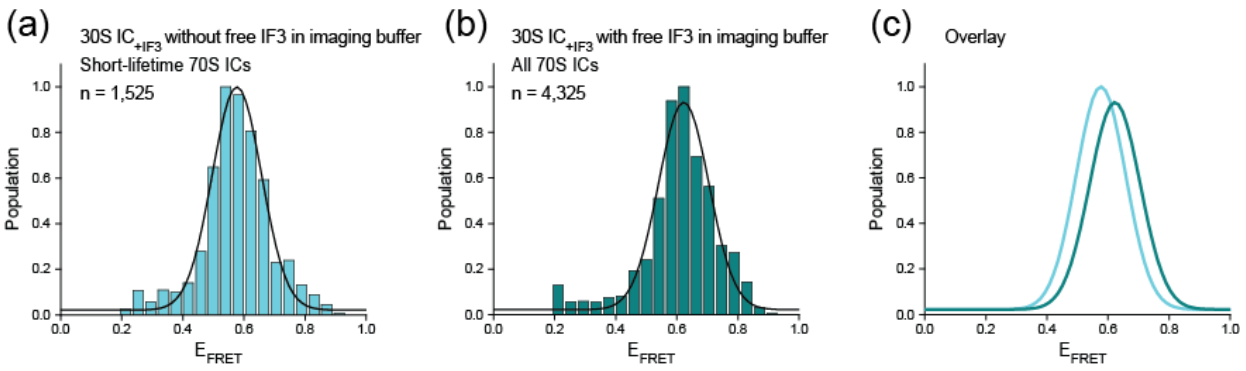

Figure S7: Short-lifetime 70S ICs are primarily formed upon subunit joining to 30S IC_{+IF3} when free IF3 is included in the imaging buffer. E_{FRET} data from subunit joining events was obtained from idealized E_{FRET} versus time trajectories (see Materials and Methods) and used to construct histograms of E_{FRET} ratios. **(a)** For 30S IC_{+IF3} without free IF3 in the imaging buffer, only data from short-lifetime 70S ICs (defined as dwells in the aggregate non-zero FRET state shorter than 4 s) were included in the histogram. The histogram was fit with a single Gaussian, which is centered at E_{FRET} = 0.58. **(b)** For 30S IC_{+IF3} with 0.9 μM free IF3 in the imaging buffer, all observed 70S ICs were included in the histogram. The histogram was fit with a single Gaussian, which is centered at E_{FRET} = 0.62. **(c)** Overlay of the fits to the two datasets. The number of 70S ICs used to construct the histograms is indicated by "n." The histograms comprise data grouped together from experiments performed at all (Cy5)50S subunit concentrations tested (10, 20, 40, and 60 nM).

Table S1: Lifetime of the aggregate non-zero FRET state observed upon subunit joining to 30S IC_{-IF3} measured using shuttering

GXP[(a)]	Shuttering Interval (s)[(b)]	τ_{nz} (s)[(c)]
GTP	0	21 ± 1
GTP	0.2	47 ± 3
GTP	0.5	47 ± 4
GTP	1	71 ± 8
GTP	2	82 ± 7
GTP	4	86 ± 8
GTP	6	120 ± 10
GDPNP	4	590 ± 40

(a) (Cy3)30S IC_{-IF3}s contained either (Cy3)IF2-GTP or (Cy3)IF2-GDPNP as indicated.

(b) Following an initial 5 s of continuous data acquisition, the laser light was shuttered and one 100 ms frame was collected per indicated time interval. The shuttering interval of 0 corresponds to continuous data acquisition at a frame rate of 10 s^{-1} for the duration of the experiment.

(c) Dwells in the aggregate non-zero FRET state subsequent to subunit joining were used to construct survival probability plots with bin widths of 15 s. These plots were fit with a single-exponential decay, the lifetime of which is reported here. The Adj. R^2 value for the fits was ≥0.93 in all cases. Values represent the mean and standard deviation obtained from bootstrapping analysis with 100 replicates.

Table S2: Lifetimes of the zero-FRET state and the aggregate non-zero FRET state for subunit joining to 30S IC_{+IF3}

(Cy5)50S (nM)	Free fMet-$tRNA^{fMet}$[a]	Lifetime of Zero-FRET State (s) [b]	Lifetime of Aggregate Non-Zero FRET State[c]			
			τ_1 (s)	A_1 (%)	τ_2 (s)	A_2 (%)
10	-	6.5 ± 0.4	0.75 ± 0.09	68 ± 4	12 ± 2	32 ± 4
20	-	4.6 ± 0.2	0.9 ± 0.1	72 ± 3	14 ± 2	28 ± 3
40	-	3.3 ± 0.2	0.7 ± 0.1	66 ± 4	11 ± 2	34 ± 4
60	-	2.9 ± 0.1	0.65 ± 0.07	64 ± 4	10 ± 1	36 ± 4
20	+	5.8 ± 0.3	0.77 ± 0.05	72 ± 3	17 ± 2	28 ± 3

(a) In these experiments, the imaging buffer delivered into the flowcell contained (Cy5)50S subunits, IF1 (0.9 μM), and GTP (1 mM). fMet-$tRNA^{fMet}$ (0.9 μM) was omitted or included as indicated.

(b) Lifetimes of the zero-FRET state were obtained by single-exponential fitting to survival probability plots as described in Materials and Methods. The Adj. R^2 value for the fit was ≥0.97 in all cases. Reported values represent the mean and standard deviation obtained from bootstrapping analysis with 100 replicates.

(c) Lifetimes of the aggregate non-zero FRET state were obtained by double-exponential fitting to survival probability plots as described in Materials and Methods. The Adj. R^2 value for the double-exponential fits was ≥0.99 in all cases; in contrast, single-exponential fits to the data had Adj. R^2 ≤0.76. Lifetimes and amplitudes for the two phases of the double-exponential decay are given. Reported values represent the mean and standard deviation obtained from bootstrapping analysis with 100 replicates.

Table S3: Lifetimes of the zero-FRET state and the aggregate non-zero FRET state for subunit joining to 30S IC_{+IF3} in the presence of free IF3

(Cy5)50S (nM)	Free fMet-tRNA^{fMet} (a)	Lifetime of Zero-FRET State (s) (b)	Lifetime of Aggregate Non-Zero FRET State (s) (c)
10	-	7.2 ± 0.4	0.89 ± 0.07
20	-	5.4 ± 0.2	0.71 ± 0.03
40	-	3.6 ± 0.1	0.63 ± 0.02
60	-	3.0 ± 0.1	0.65 ± 0.02
20	+	6.6 ± 0.2	0.56 ± 0.03

(a) In these experiments, the imaging buffer delivered into the flowcell contained (Cy5)50S subunits, IF1 (0.9 μM), IF3 (0.9 μM), and GTP (1 mM). fMet-tRNA^{fMet} (0.9 μM) was omitted or included as indicated.

(b) Lifetimes of the zero-FRET state were obtained by single-exponential fitting to survival probability plots as described in Materials and Methods. The Adj. R^2 value for the fit was ≥0.99 in all cases. Reported values represent the mean and standard deviation obtained from bootstrapping analysis with 100 replicates.

(c) Lifetimes of the aggregate non-zero FRET state were obtained by single-exponential fitting to survival probability plots as described in Materials and Methods. The Adj. R^2 value for the fit was ≥0.92 in all cases. Reported values represent the mean and standard deviation obtained from bootstrapping analysis with 100 replicates.

Table S4: Lifetimes of the zero-FRET state and the aggregate non-zero FRET state for subunit joining to 30S IC_{+IF3} with different concentrations of IF3 in the imaging buffer

Free IF3 (nM)[(a)]	Lifetime of Zero-FRET State (s)[(b)]	Lifetime of Aggregate Non-Zero FRET State[(c)]			
		τ_1 (s)	A_1 (%)	τ_2 (s)	A_2 (%)
0	5.9 ± 0.2	0.84 ± 0.09	67 ± 2	21 ± 2	33 ± 2
9	6.5 ± 0.3	0.92 ± 0.08	69 ± 2	22 ± 2	31 ± 2
90	5.7 ± 0.3	0.91 ± 0.09	68 ± 2	22 ± 2	32 ± 2
900	6.3 ± 0.3	0.77 ± 0.05	--	--	--

(a) In these experiments, the imaging buffer delivered into the flowcell contained (Cy5)50S subunits (20 nM), IF1 (0.9 μM), GTP (1 mM), and IF3 at the indicated concentrations. IF3 was serially diluted before adding to the imaging buffer, and smFRET data for all four titration points was collected on the same day and under the same experimental conditions.

(b) Lifetimes of the zero-FRET state were obtained by single-exponential fitting to survival probability plots as described in Materials and Methods. The Adj. R^2 value for the fit was ≥0.99 in all cases. Reported values represent the mean and standard deviation obtained from bootstrapping analysis with 100 replicates.

(c) Lifetimes of the aggregate non-zero FRET state were obtained by exponential fitting to survival probability plots as described in Materials and Methods. Single-exponential fitting yielded Adj. R^2 values of 0.56, 0.57, and 0.56 for datasets with 0, 9, and 90 nM free IF3 respectively. The dataset with 900 nM free IF3 was fit significantly better than the rest with a single-exponential (Adj. R^2 = 0.88), and the lifetime thus obtained is given here. The datasets with 0, 9, and 90 nM free IF3 required double-exponential fitting, and the lifetimes and amplitudes for the two phases of the decay are given here. Adj. R^2 values for double-exponential fitting were ≥0.99 in all cases. Reported lifetimes and amplitudes represent the mean and standard deviation obtained from bootstrapping analysis with 100 replicates.

Table S5: Lifetimes of the zero-FRET state and the aggregate non-zero FRET state for subunit joining to 30SIC$_{+IF3(Y75N)}$

Free IF3(Y75N)[(a)]	Lifetime of Zero-FRET State (s) [(b)]	Lifetime of Aggregate Non-Zero FRET State[(c)]			
		τ_1 (s)	A_1 (%)	τ_2 (s)	A_2 (%)
-	4.1 ± 0.2	1.9 ± 0.3	56 ± 4	21 ± 2	44 ± 4
+	5.8 ± 0.3	0.76 ± 0.05	85 ± 2	17 ± 3	15 ± 2

(a) In these experiments, the imaging buffer delivered into the flowcell contained (Cy5)50S subunits (20 nM), IF1 (0.9 μM), and GTP (1 mM). IF3(Y75N) (0.9 μM) was omitted or included in the imaging buffer as indicated.

(b) Lifetimes of the zero-FRET state were obtained by single-exponential fitting to survival probability plots as described in Materials and Methods. The Adj. R^2 value for the fit was ≥0.99 for both datasets. Reported values represent the mean and standard deviation obtained from bootstrapping analysis with 100 replicates.

(c) Lifetimes of the aggregate non-zero FRET state were obtained by double-exponential fitting to survival probability plots as described in Materials and Methods. The Adj. R^2 value for the double-exponential fits was ≥0.99 for both datasets. Single-exponential fits to the data yielded Adj. R^2 values of 0.83 and 0.76 for the datasets with and without free IF3(Y75N) in solution, respectively. Lifetimes and amplitudes for the two phases of the double-exponential decay are given. Reported values represent the mean and standard deviation obtained from bootstrapping analysis with 100 replicates.

REFERENCES

1. Elvekrog, M. M. & Gonzalez, R. L., Jr. (2013). Conformational selection of translation initiation factor 3 signals proper substrate selection. *Nat Struct Mol Biol* **20**, 628-33.
2. Fei, J., Wang, J., Sternberg, S. H., MacDougall, D. D., Elvekrog, M. M., Pulukkunat, D. K., Englander, M. T. & Gonzalez, R. L., Jr. (2010). A highly purified, fluorescently labeled in vitro translation system for single-molecule studies of protein synthesis. *Methods Enzymol* **472**, 221-59.
3. Bowen, W. S., Van Dyke, N., Murgola, E. J., Lodmell, J. S. & Hill, W. E. (2005). Interaction of thiostrepton and elongation factor-G with the ribosomal protein L11-binding domain. *J Biol Chem* **280**, 2934-43.
4. Van Dyke, N., Xu, W. & Murgola, E. J. (2002). Limitation of ribosomal protein L11 availability in vivo affects translation termination. *J Mol Biol* **319**, 329-39.
5. Brandi, L., Marzi, S., Fabbretti, A., Fleischer, C., Hill, W. E., Gualerzi, C. O. & Stephen Lodmell, J. (2004). The translation initiation functions of IF2: targets for thiostrepton inhibition. *J Mol Biol* **335**, 881-94.
6. Weinger, J. S., Parnell, K. M., Dorner, S., Green, R. & Strobel, S. A. (2004). Substrate-assisted catalysis of peptide bond formation by the ribosome. *Nat Struct Mol Biol* **11**, 1101-6.